Complete ^1H, ^{13}C, and ^{15}N Assignments and Secondary Structure of the GTPase Activating Domain of G_s†

Dennis R. Benjamin,‡ David W. Markby,§ Henry R. Bourne,§ and Irwin D. Kuntz*,‡

Departments of Pharmaceutical Chemistry and Pharmacology, University of California at San Francisco, San Francisco California 94143

Received August 25, 1994; Revised Manuscript Received October 13, 1994⊗

ABSTRACT: Complete ^1H, ^{13}C, and ^{15}N assignments for backbone and side-chain atoms of the 145 residue GTPase activating domain of G_s are presented. The combination of gradient-enhanced versions of the HNCACB and CBCA(CO)NNH pulse sequences provided enough information to obtain sequential backbone assignments for residues 2−145 of the polypeptide, as well as assignments of asparagine and glutamine side-chain amides. HBHA(CO)NNH, HCCH-TOCSY, and $^{13}C/^{15}N$ NOESY-HSQC experiments yielded side-chain ^1H and ^{13}C assignments. Chemical shift data and ^{15}N NOESY-HSQC experiments provided information on the secondary structure of the domain, which is similar to that observed in the cognate domain in transducin, a related G protein. The functionally essential C-terminal 15 residues are disordered in solution. These assignments provide a basis for determining the solution structure of the domain.

The GTPase[1] superfamily comprises a diverse array of signal-transducing and regulatory proteins which couple hydrolysis of GTP to the regulation of processes ranging from protein synthesis to vision and olfaction (Birnbaumer et al., 1987; Bourne et al., 1991; Simon et al., 1991). The GTP binding cores of all these proteins hydrolyze GTP and share primary and tertiary structure similarity. Members of the family also share a common molecular mechanism. The active, GTP-bound form of the molecule binds to downstream effectors and regulates their activity. Slow hydrolysis of bound GTP converts the enzyme to an inactive, GDP-bound form. Guanine nucleotide release proteins (GNRPs) catalyze release of bound GDP, allowing its replacement by GTP and reactivation of the GTPase.

Cells regulate the ratio of active and inactive GTPases at two steps in this cycle: GDP release and GTP hydrolysis. Guanine dissociation inhibitors hinder GDP release and maintain GTPases in the inactive form, while GNRPs accelerate GDP release, shifting the equilibrium in favor of the active form. At the other end of the cycle, GTPase activating proteins (GAPs) accelerate the rate of GTP hydrolysis, reducing the active state population. For small GTPases (e.g., ras-like GTPases and elongation factors), regulation of these sorts is carried out by separate gene products.

The heterotrimeric G proteins are a subfamily of GTPases which couple activation of serpentine receptors (transmembrane receptors having seven membrane-spanning helices) to the regulation of ion channels and intracellular enzymes. For example, the α chain of G_s (α_s) couples activation of β adrenergic and other receptors to stimulation of adenylyl cyclase. The α subunits of G proteins (G_α) contain the GTP-binding core common to the GTPase family but are distinguished by an insertion of ~140 residues in a loop known to be a site of GAP binding to small GTPases. Additionally, G_α proteins hydrolyze GTP at a relatively constant rate which is 2 orders of magnitude greater than that of other GTPases. These observations prompted the hypothesis that the inserted domain acts as a built-in GAP (Freissmuth & Gilman, 1989; Landis et al., 1989), a hypothesis supported by the recent demonstration that the inserted domain, when expressed as a separate protein, can stimulate GTP hydrolysis in the GTPase core of α_s (Markby et al., 1993). We refer to the inserted domain as Gail (GAP-like), and to the GTP-binding core as Ralph (Ras-like).

The Ralph domains of G proteins show substantial similarity in both their primary and tertiary structures. The Gail domains show less similarity in sequence and are not present in the two GTPases (Ras and EF-Tu) first crystallized (Jurnak, 1985; Milburn et al., 1990; Pai et al., 1990). A crystal structure for the α chain (α_t) of the phototransducing heterotrimeric G protein G_t has been recently reported (Noel et al., 1993). While this provides a first look at the structure of a Gail domain, α_t has only 22% sequence identity with α_s in this region, and thus some differences might be expected between the two proteins. Further interesting differences may arise from the intermolecular nature of the Ralph/Gail interactions in our model system. In order to elucidate the solution structure of the Gail domain of G_s and study its role in regulating GTPase activity, we have undertaken heteronuclear NMR studies of isotopically labeled recombinant protein.

EXPERIMENTAL PROCEDURES

Sample Preparation. A polypeptide comprising amino acids 84−219 of the long splice variant (Robishaw et al.,

†These studies were supported by NIH Grants GM 27800 and GM 31497, an NSF Graduate Fellowship (D.R.B.), and an NIH NRSA Postdoctoral Fellowship (D.W.M.).

* To whom correspondence should be addressed.

‡Department of Pharmaceutical Chemistry.

§ Department of Pharmacology.

⊗ Abstract published in *Advance ACS Abstracts,* December 1, 1994.

[1] Abbreviations: GTPase, guanosine-5′-triphosphatase; NMR, nuclear magnetic resonance; GTP, guanine triphosphate; GDP, guanosine diphosphate; GNRP, guanine nucleotide release protein; GAP, GTPase activating protein; SDS−PAGE, sodium dodecyl sulfate−polyacrylamide gel electrophoresis; NOE, nuclear Overhauser effect

0006-2960/95/0434-155$09.00/0

1986) of α_s was overexpressed in *Escherichia coli* BL21-(DE3) pLysS. The version of Gail used in this study included a 10-residue monoclonal antibody epitope at the N-terminus. ^{15}N and ^{13}C were incorporated into the protein by growing cells in a minimal medium with 1 g/L $(^{15}NH4)_2SO_4$ and 2 g/L uniformly labeled [^{13}C]glucose as the sole nitrogen and carbon sources, respectively. Cells were grown at 37 °C to an OD_{600} of 0.8, and protein expression was induced by addition of isopropyl thiogalactoside. The cells were harvested 4 h after induction by centrifugation and frozen at −80 °C. The recombinant protein was purified using anion exchange, gel filtration, and hydroxylapatite chromatographies as described previously (Markby et al., 1993). Protein purity was estimated at >98% by SDS−PAGE and 2D NMR spectroscopy. Samples (1−3mM) were exchanged into 10 mM sodium phosphate, 10 mM DTT, 0.01% NaN_3, and 10% ^2H_2O at a pH of 6.0 using Centricon 10 concentrators. Protein concentration was determined by measuring OD_{280}.

NMR Spectroscopy. All NMR spectra were recorded at 30 °C using samples prepared in H_2O buffers only, on a Varian Unity+ 600 MHz spectrometer equipped with an actively shielded triple-resonance (^1H,^{13}C,^{15}N) probe and pulsed field gradients. Carrier frequencies were typically 4.74 ppm for ^1H, 119 ppm for ^{15}N, 43 ppm for aliphatic ^{13}C, 56 ppm for ^{13}Ca, and 177 ppm for $^{13}C'$. All amide-proton detected experiments used the gradient-enhanced method described by Kay et al. (1992), which provides both coherence transfer selection and solvent suppression. In order to avoid saturation of amide resonances by spin diffusion or chemical exchange (Grzesiek & Bax, 1993b), no presaturation or spin-lock purging pulses (Messerle et al., 1989) were employed. Two-dimensional $^{15}N-^1H$ HSQC (Bodenhausen & Ruben, 1980) spectra were acquired with the pulse sequence described by Kay et al. (1992). CBCA-(CO)NNH, HNCACB, and HNCO spectra were acquired using modified sequences (Muhandiram et al., 1993) which incorporate pulsed field gradients and constant time acquisition periods. The CBCA(CO)NNH experiment was modified to record $^1H\alpha$ and $^1H\beta$ chemical shifts, yielding an HBHA-(CACO)NNH experiment (Grzesiek & Bax, 1993a). HCCH-TOCSY spectra were acquired using the pulse sequence of Kay et al. (1993) designed for use with samples in H_2O; two spectra were recorded, using mixing periods of 8 ms (providing neighboring connectivities only) and 16 ms (correlating entire spin systems). A ^{15}N NOESY-HSQC spectrum was acquired using a modified NOESY-HMQC experiment (Marion et al., 1989a) which incorporates a semiconstant time refocused HSQC transfer for ^{15}N chemical shift detection and gradients for coherence selection. A 100-ms mix time was used. A $^{13}C/^{15}N$ NOESY-HSQC experiment (Pascal et al., 1994) was recorded, which uses a shared frequency-labeling period to obtain both ^{13}C and ^{15}N chemical shifts in the third dimension. The number of complex points and acquisition times for all experiments were as follows: for $^{15}N-^1H$ HSQC, ^{15}N (F_1), 256 points, 128 ms; ^1H (F_2), 2048 points, 250 ms; for HNCACB, ^{15}N (F_1), 32 points, 16 ms; ^{13}C (F_2), 64 points, 98 ms; ^1H (F_3), 1024 points, 120 ms; for CBCA(CO)NNH, ^{15}N (F_1), 32 points, 16 ms; ^{13}C (F_2), 64 points, 11 ms; ^1H (F_3), 1024 points, 120 ms; for HNCO, ^{15}N (F_1) 32 points, 16 ms; $^{13}C'$ (F_2), 64 points, 18 ms; ^1H (F_3), 1024 points, 120 ms; for HBHA-(CACO)NNH, ^{15}N (F_1), 32 points, 16 ms; ^1H (F_2), 128 points, 30 ms; ^1H (F_3), 1024 points, 120 ms; for HCCH-TOCSY, ^{13}C (F_1), 64 points, 10.5 ms; ^1H (F_2), 128 points, 38 ms; ^1H (F_3), 1024 points, 230 ms; for ^{15}N NOESY-HSQC, ^{15}N (F_1), 24 points, 20 ms; ^1H (F_2), 128 points, 24 ms; ^1H (F_3), 1024 points, 120 ms; for $^{13}C/^{15}N$ NOESY-HSQC, $^{13}C/^{15}N$ (F_1), 64 points, 11 ms; ^1H (F_2), 128 points, 24 ms; ^1H (F_3), 1024 points, 120 ms. For all indirect dimensions, States−TPPI phase cycling was used for quadrature detection (Marion et al., 1989c), and 180° linear phase corrections were obtained by setting initial time increments to half a dwell period (Bax et al., 1991).

Data Processing. Spectra were processed using both the in-house program Striker (Day, unpublished) and the nmrPipe suite of programs (Delaglio, unpublished). For gradient-enhanced NH detected spectra (all but the $^{13}C/^{15}N$ HSQC NOESY and the HCCH-TOCSY), States-type hypercomplex data were generated by postacquisition data processing according to the procedure of Kay et al. (1992), and solvent suppression was enhanced via time-domain convolution (Marion et al., 1989b). Spectra were apodized via multiplication by shifted sine bells and zero filled once prior to Fourier transformation. All 3D spectra were extended in t_1 prior to zero-filling by forward−backward linear prediction (Zhu & Bax, 1992). Analysis and assignments were performed using the interactive software package Sparky, written in-house (Kneller, unpublished). Chemical shift indices were calculated with the program CSI (Wishart & Sykes, 1994).

RESULTS

2D HSQC. Figure 1 shows a two-dimensional $^{15}N-^1H$ HSQC spectrum of Gail. Despite the low amide proton dispersion, there are no absolutely degenerate signals. There are two cases of near degeneracy, F136/K139 and R88/V42, but the ^{15}N chemical shifts of these residues are sufficiently distinct to allow unambiguous assignment in 3D spectra. Additionally, all five arginyl ϵ-amino groups are resolved, as are all 14 glutamine and asparagine side-chain amides. The N-terminal 12 residues and C-terminal 15 residues have intense signals and narrow line widths in this spectrum, indicating that they are more mobile than the rest of the protein.

Aqueous NMR samples typically contain 10% D_2O, added for field-frequency locking. This spectroscopically invisible D_2O chemically exchanges with labile protons (e.g., NH, OH) in the protein and results in a slight attentuation of signals arising from backbone amide protons. In the case of Asn and Gln side chains, however, this exchange generates an NHD group. These species are still visible in HSQC spectra by virtue of their single attached proton, but the one-bond deuterium isotope effect shifts their ^{15}N frequency 0.5 ppm upfield relative to the NH_2 group. Weak cross peaks deriving from this exchange are marked by asterisks in Figure 1. Their rates of appearance vary for different residues in spectra of Gail taken over a 3 week period and thus provide an indicator of hydrogen bonding in side chains. The cross peaks are also useful in assigning side-chain amide protons to specific residues (vide infra).

Assignment Strategy. The original procedure proposed by Ikura et al. (1990) for assigning heteronuclear spectra of proteins requires a minimum of five separate experiments, because each experiment provides only a single interresidue

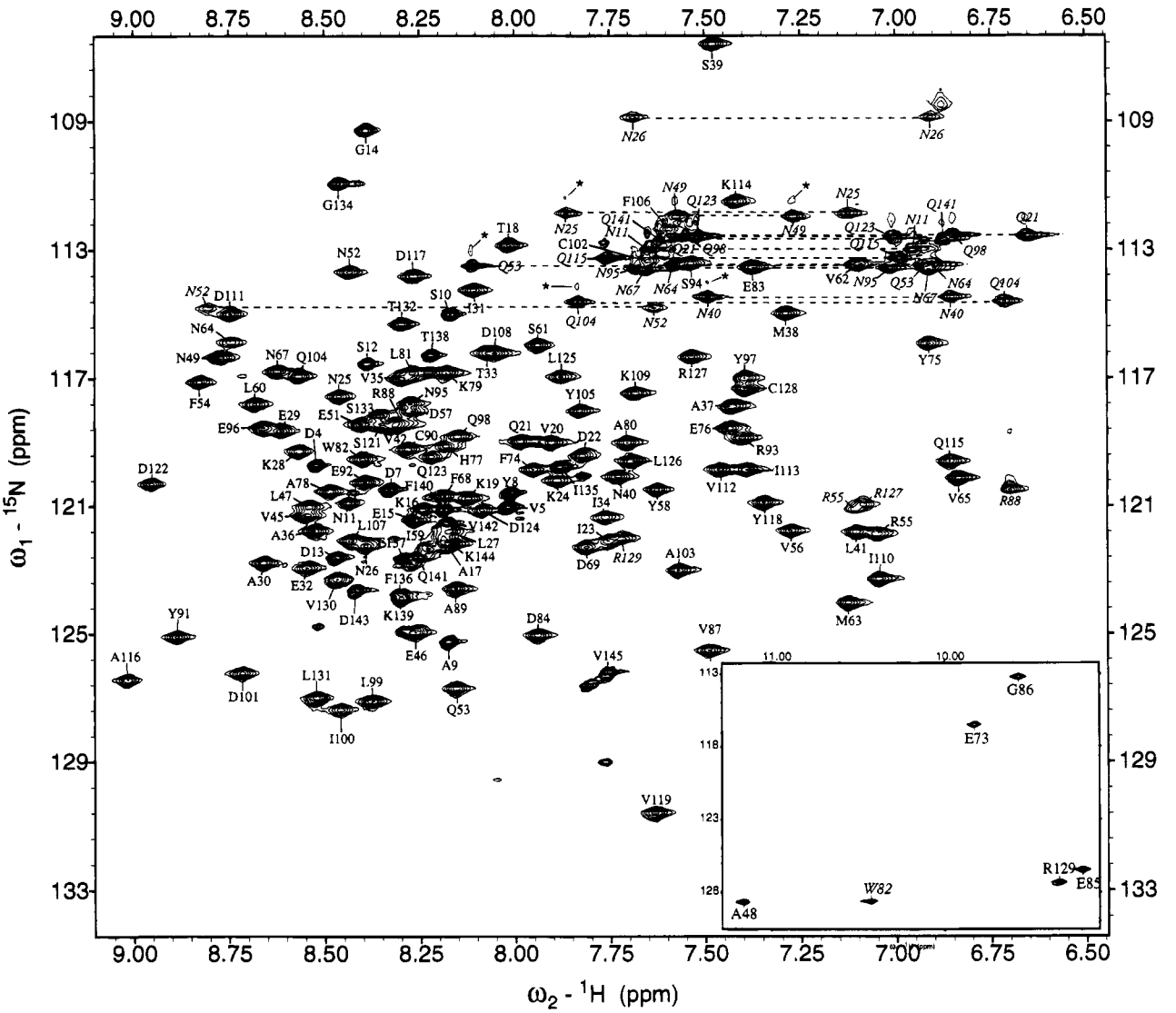

FIGURE 1: ^{15}N−^{1}H HSQC of G_s Gail. Labels for cross peaks arising from Asn, Gln, Trp, and (folded) Arg side chain, are italicized. Asterisks indicate peaks arising from monodeuterated Asn and Gln side chain amides.

correlation (e.g., Hα). More recently, the introduction of the CBCA(CO)NNH (Grzesiek & Bax, 1992) and HNCACB (Wittekind & Mueller, 1993) experiments has allowed a simpler protocol, often requiring only these two experiments (Anglister et al., 1994; Garrett et al., 1994). By providing both Cα and Cβ chemical shifts of neighboring residues, the experiments lift the ambiguity present in, e.g., the HNCA/HNCOCA combination caused by degenerate Cα frequencies. The loss in sensistivity associated with obtaining the extra information did not pose a problem for the 16-kDa Gail domain.

In order to assign the backbone resonances of Gail, these two experiments were first used to link together strings of neighboring amino acids. The HNCACB correlates the amide proton and nitrogen of a given residue with the intraresidue Cα and Cβ, while the CBCA(CO)NNH provides correlations to the Cα and Cβ of the preceding residue. By alternating between the two spectra, one can establish the connectivity of amide cross peaks in a 2D HSQC spectrum. This procedure is demonstrated in Figure 2. The connections between Y97, Q98, and L99 illustrate the importance of the Cβ chemical shift in distinguishing between residues having degenerate Cαs; the Cα chemical shift of the residue preceding L99 could correspond to either Q98 or Y97. Additionally, this section illustrates the value of the HNCACB's property of recording Cα and Cβ chemical shifts 180° out of phase; the Cα and Cβ resonances of S94 would otherwise be difficult to distinguish.

After connecting together all cross peaks present in the HSQC spectrum, the unique Cβ chemical shifts of Ala, Ser, and Thr and the lack of a Cβ in Gly identified these species in the strings of connected residues and yielded an unambiguous mapping back to the amino acid sequence. The HBHA(CACO)NNH spectrum provided Hα and Hβ frequencies, completing the assignment process for Ala, Gly, Asn, Asp, Cys, and Ser. HCCH-TOCSY experiments provided aliphatic side-chain assignments for other residues; data from residue I100 are shown in Figure 3 to illustrate the quality of the 16-ms spectrum. Almost all of the side chains in Gail have been assigned; exceptions include K139 and K144, and V130 and V142, which are entirely degenerate, preventing unique assignment of ^{13}C frequencies.

The dephasing period of the final ^{15}N → ^{1}H transfer of the CBCA(CO)NNH experiments is tuned for NH groups and selects against NH_2 groups; thus, no cross peaks from Asn or Gln side chain amides are present in the spectrum.

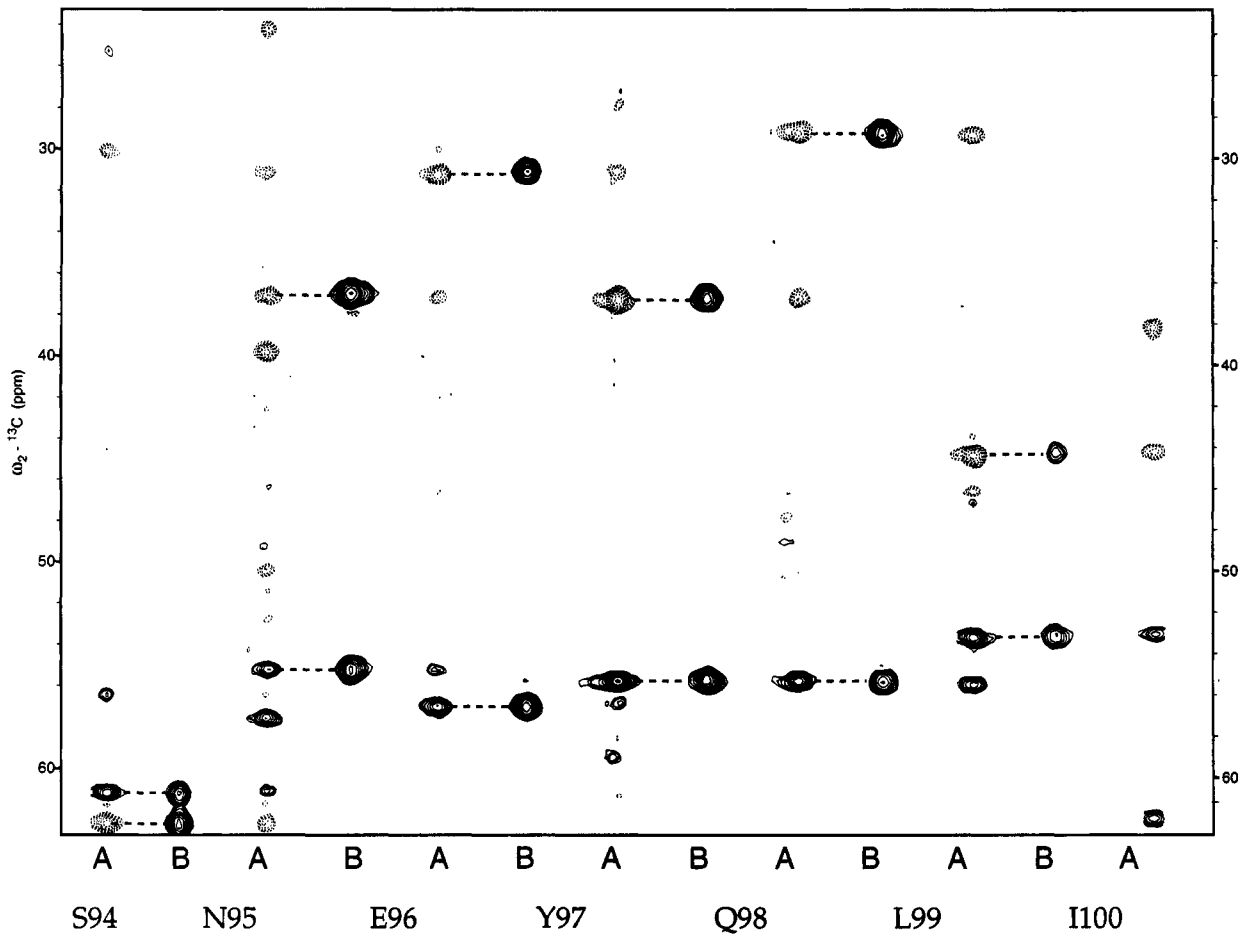

FIGURE 2: Strips extracted from HNCACB (A) and CBCA(CO)NNH (B) spectra, showing residues S94–I100. Dashed contours are used for negative peaks. Dashed lines indicate sequential Cα and Cβ connectivities.

However, NHD groups arising from chemical exchange with D_2O (vide supra) behave spectroscopically as NH groups and do yield correlations between side-chain amide protons and nitrogens and either Asn Cαs and Cβs or Glu Cβs and Cγs. These correlations (occurring at ^{15}N frequencies 0.5 ppm upfield of the NH_2 ^{15}N chemical shift) allowed the specific assignment of all side chain amides in Gail; Figure 4 shows the region of the CBCA(CO)NNH spectrum containing correlations for side chains of residues Q21, Q98, Q123, and Q141.

The finite bandwidth of the DIPSI-3 mixing sequence in HCCH-TOCSY experiments prevents any coherence transfer to aromatic carbons; therefore, aromatic side-chain assignments were obtained from the 3D $^{13}C/^{15}N$ HSQC-NOESY. This experiment records NOEs to both ^{13}C-attached and ^{15}N-attached protons, and therefore yields NOEs from side-chain protons to the HNε of Arginine groups, allowing their assignment.

Table 1, containing a list of the chemical shifts of all ^1H, ^{13}C, and ^{15}N atoms, is available as supplementary material.

Secondary Structure. Regular secondary structural elements in proteins give rise to characteristic interresidue distances (Wüthrich, 1986); these short-range distances can be identified in NOE spectra and used to delineate the beginning and end of such elements. Of particular relevance to this protein are the short distances found in α-helices, including NH(i)–NH(i+1), NH(i)–NH(i+2), Hα(i)–NH(i+3), Hα(i)–NH(i+4), and Hα(i)–Hβ(i+3). α-Helices are also characterized by weak or absent Hα(i)–NH(i+1) cross peaks. Additionally, chemical shifts of backbone atoms (Cα, Cβ, Hα, C′) are powerful predictors of the presence of secondary structure (Spera & Bax, 1991; Wishart et al., 1991). Wishart and Sykes (1994) have recently described a chemical shift consensus index, calculated from all four backbone atoms, which predicts secondary structures with an accuracy greater than 90%. Lastly, amide protons of residues involved in helices and sheets are typically protected from chemical exchange with solvent and can be identified by substituting D_2O for H_2O in the buffer. Figure 5 summarizes short- and medium-range NOEs observed, the chemical shift index, exchange-protected amides, and predicted regions of α-helix within Gail.

DISCUSSION

CD spectra and preliminary 3D ^{15}N NOESY-HMQC spectra of ^{15}N single labeled protein led to the prediction that the secondary structure of the Gail domain of G_s consisted largely or exclusively of α-helices (D. Markby and D. Benjamin, unpublished results); this prediction is supported by the crystal structure of transducin. Helical proteins are characterized by poor chemical shift dispersion in both the amide and the α proton regions; this degeneracy complicates the assignment procedure by introducing substantial overlap. Gail is no exception to this rule, with 92% of all amide and 85% of all alpha protons falling within 1.8 ppm ranges. Despite this handicap, isotopic labeling of the protein afforded sufficient extra resolution to enable virtually

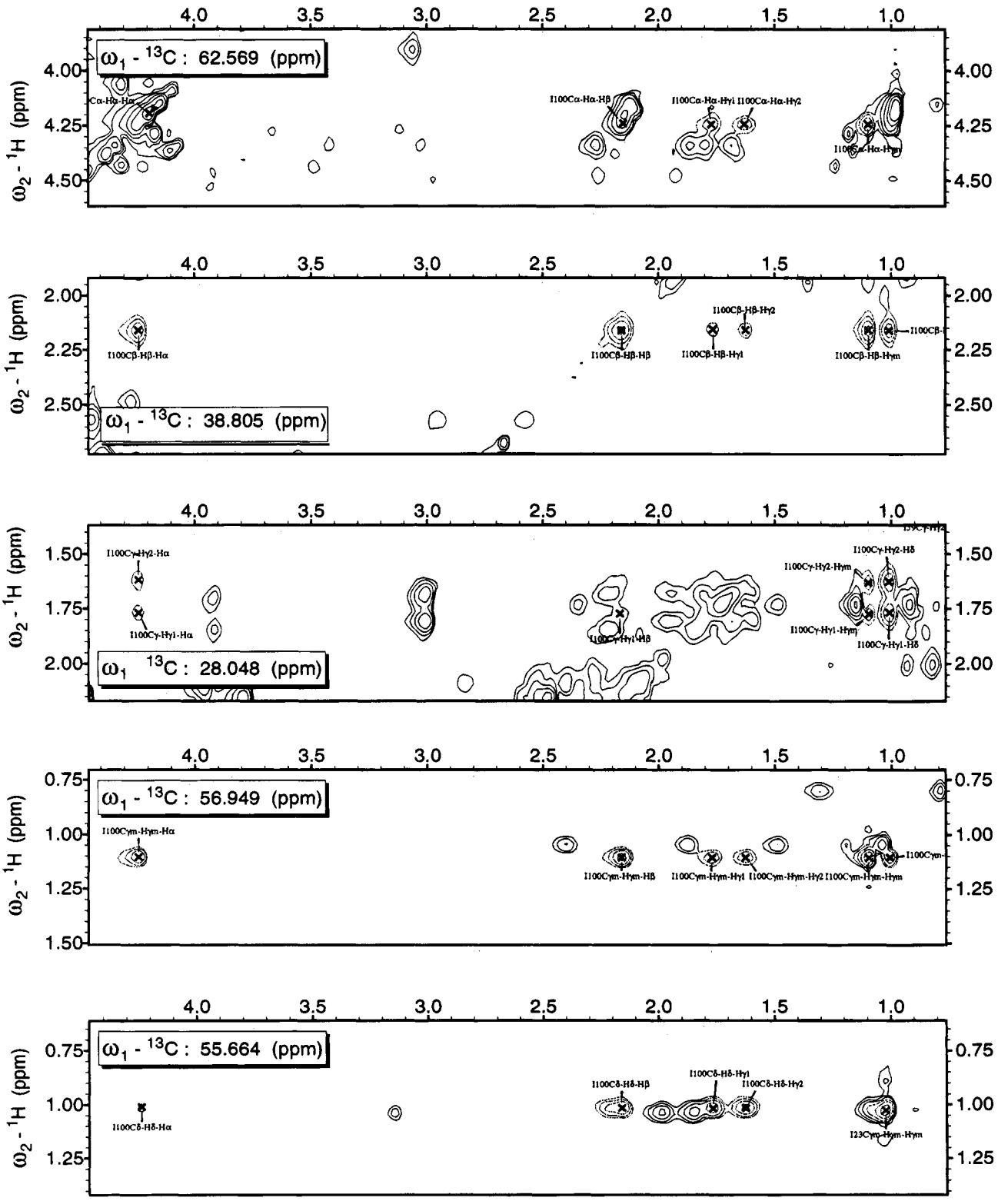

FIGURE 3: Series of F_2,F_3 strips extracted from the 16-ms HCCH-TOCSY spectrum at ^{13}C (F1) chemical shifts of I100 Cα, Cβ, Cγ, Cγm, and Cδ.

complete assignment of the entire molecule. The use of pulsed-field gradients for coherence selection and artifact suppression enhanced sensitivity in NH-detected experiments and minimized the required phase cycles. The reduced phase cycles in particular allowed acquisition of high-resolution data in indirect dimensions.

The line widths in 2D $^{15}N-^{1}H$ HSQC spectra and the NOEs observed in various 3D NOE spectra indicate that Gail is monomeric and structured in solution. This is consistent with our previous demonstration of Gail's ability to accelerate slow GTP hydrolysis in a separately expressed Ralph domain (Markby et al., 1993). It is also consistent with the observation in the crystal structure of α_t that the Gail and Ralph domains have few contacts and the prediction that guanine nucleotide exchange is mediated by "en bloc" movement of the rigid Gail domain (Noel et al., 1993).

The secondary structure of α_s Gail consists entirely of helices, identified by contiguous stretches of Hα(i)−Hβ(i+3),

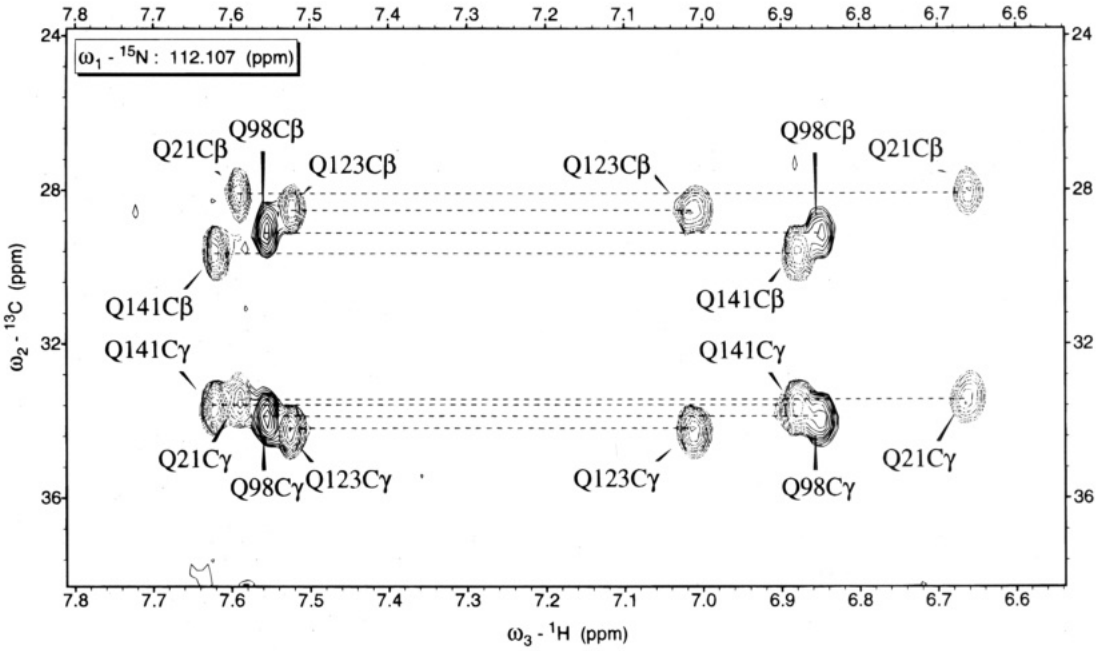

FIGURE 4: Region of CBCA(CO)NNH spectrum showing glutamine Cα and Cβ correlations to monodeuterated side-chain amides (NHD). The cross peaks appear in the 3D spectrum at a ^{15}N chemical shift 0.5 ppm upfield of the NH_2 cross peaks in the HSQC spectrum (Figure 1).

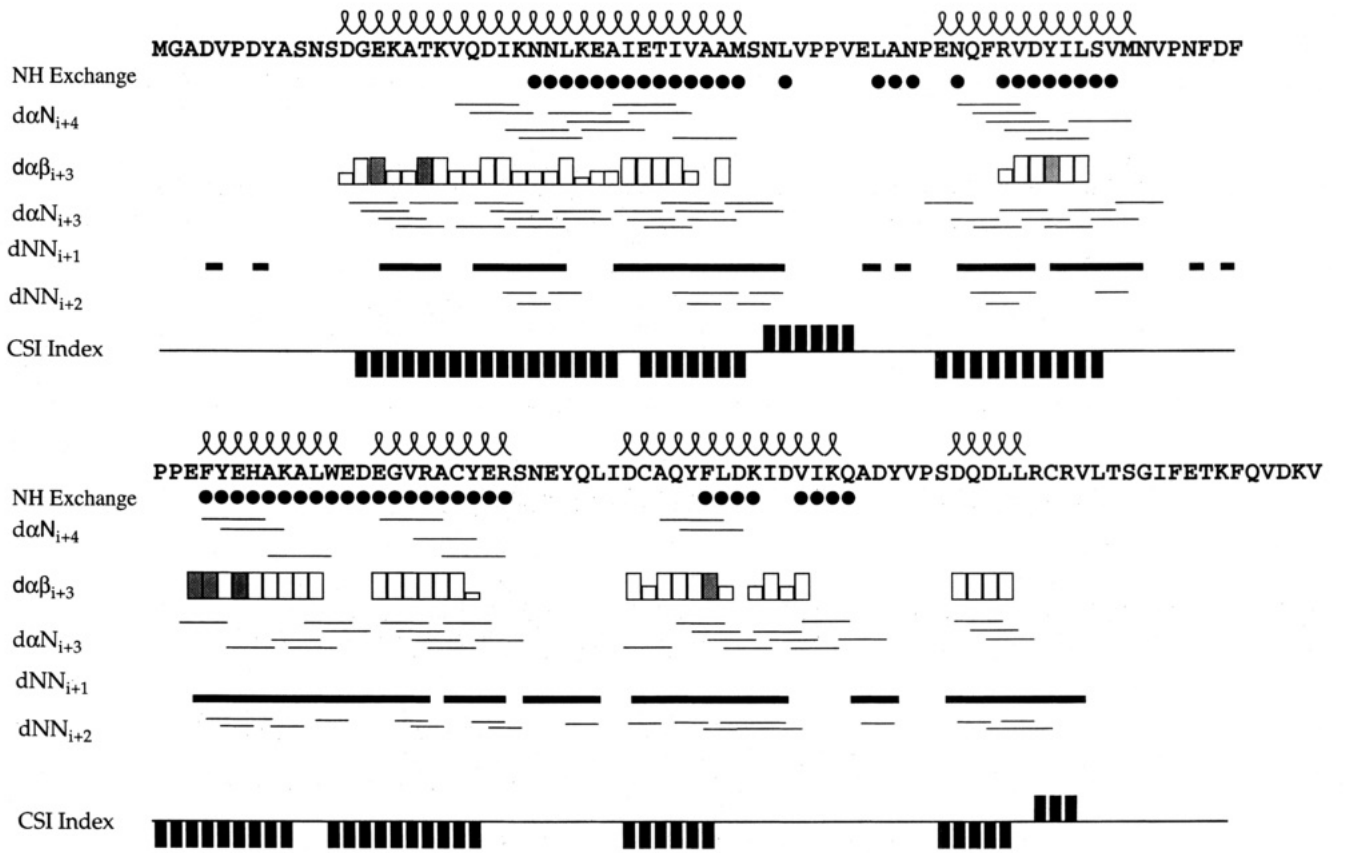

FIGURE 5: Primary sequence of G_s Gail with a summary of observed short- and medium-range NOEs, hydrogen exchange data, and the chemical shift index (Wishart & Sykes, 1994). Circles below the sequence indicate residues with amide protons still visible in a 2D HSQC spectrum after 36 h of solvent exchange in D_2O buffer at pH 6.0, 10 °C.

HN(i)−HN(i+1), and Hα(i)−NH(i+3) NOEs, along with weaker HN(i)−HN(i+2) and Hα(i)−HN(i+4) NOEs. The protein is denatured by lyophilization. This instability prevented rapid measurement of amide exchange rates to identify helix termini. The D_2O buffer exchange scheme employed required 36 h, leaving only the 56 most strongly protected amide protons. Nevertheless, analysis of NOE data in concert with the chemical shift index of Wishart and Sykes yielded a reliable delineation of the helices.

The first 12 amino acids of Gail, which include a 10 residue epitope, show only a few, weak NOEs, narrow line widths and are presumably unstructured in solution. The presence of an Hα(i)−NH(i+3) NOE at D13 indicates the start of a long helix which continues through to N40. A

break in the CSI consensus index, along with a weakening of short-range NOEs, suggests that this helix is bent or otherwise perturbed around I31. The second helix starts at N52 and ends at M63. Overlap in both Hα/Cα and Hβ/Cβ impedes precise identification of the start of the next helix, but Y75 is clearly in a helical conformation. The absence of an NOE between the Hα of P71 and the Hβ of F74 indicates that P71 is not in a helix; however, prolines are observed at the N-termini of helices, suggesting that P72 might mark the start of the third helix. This helix extends to D83. A two-residue intervention is then followed at E85 by the fourth helix, which ends at S94. The next helix appears to stretch from residue Q104 to K114; however, the absence of expected NOEs between D108 and D111, along with weakness of NOEs at neighboring residues, suggests that the helix is distorted or engaged in conformational exchange. Interestingly, this is the only region where there is disagreement between the CSI and the NOEs. The last helix extends from D122 to R127 and appears to be less stable than the others as it does not show any amide exchange protection. The CSI also predicts two short regions of β-sheet; however, neither interstrand Hα−NH nor strong Hα(i)−HN(i+1) NOEs were observed to support their existence.

The six helices observed in α_s Gail correspond with those observed in the Gail domain of α_t, although there are some noticeable differences. The N-terminus of the Gail domain of α_t has a striking, long central helix around which the other helices are organized. This long helix is clearly present in α_s; however, no perturbation at I31 is evident in α_t. Helices B, C, D, and F appear to be identical in α_s and α_t, both in sequential location and in length. Helix E, however, is either shorter or distorted in α_s. As in α_t, there is no evidence for β-sheets in α_s Gail.

The C-terminal 15 amino acids are absolutely required for Gail to complement Ralph, despite the fact that this region is also present in the Ralph construct (Markby et al., 1993). This tract includes several residues which participate in electrostatic interactions with both the catalytically required magnesium ion and the triphosphate portion of GTP-γS. It is clear from both the line widths in the 2D $^{15}N-^{1}H$ HSQC and the paucity of NOEs involving these residues that they are unstructured in the isolated domain. Such C-terminal flexibility has been noted in a number of NMR studies of protein structure (Anglister et al., 1994; Lycksell et al., 1994). These studies have also shown that flexible C-termini rigidify upon binding to a partner protein, and this mechanism has been proposed to enhance the rate of specific interactions between macromolecules (Pontius, 1993).

In the crystal structure of α_t, the last 10 residues of the C-terminus of Gail form β strand 2 and loop 3; β strand 3 is present in the Ralph domain. We postulate that in in vitro interactions between Gail and Ralph, the residues in Gail displace some or all of the corresponding residues in Ralph, forming the β sheet, binding to the guanine nucleotide, and stabilizing the Gail−GTP−Ralph ternary complex. This hypothesis can be tested by studying the structure of the C-terminus of Gail in a complex of labeled Gail with unlabeled Ralph.

CONCLUSIONS

The Gail domain of α_s, expressed as an isolated polypeptide, is stable and structured in solution. Its secondary structure appears quite similar to that of α_t, as expected from the conservation of function between the two proteins. The complete assignment of the domain sets the stage for the determination of its solution structure, which will provide additional insight into the mechanisms of GTP hydrolysis and GDP release in this important family of proteins. Additionally, these assignments provide a basis for investigating the structure and dynamics of the ternary Gail−GTP−Ralph complex.

ACKNOWLEDGMENT

We are grateful to Mark Day, Frank Delaglio, Don Kneller, and David Wishart for providing software. We especially thank Lewis E. Kay for many helpful discussions and for providing most of the pulse sequences used in this study. We also thank Vladimir Basus for advice and assistance.

SUPPLEMENTARY MATERIAL AVAILABLE

^{1}H, ^{13}C, and ^{15}N assignments for all 145 residues of Gail (11 pages). Ordering information is given on any current masthead page

REFERENCES

Anglister, J., Grzesiek, S., Wang, A. C., Ren, H., Klee, C. B., & Bax, A. (1994) *Biochemistry 33*, 3540−3547.

Bax, A., Ikura, M., Kay, L. E., & Zhu, G. (1991) *J. Magn. Reson. 91*, 174−178.

Birnbaumer, L., Codina, J., Mattera, R., Yatani, A., Scherer, N., Toro, M. J., & Brown, A. M. (1987) *Kidney Int. (Suppl.) 32*, S14−S37.

Bodenhausen, G., & Ruben, D. J. (1980) *Chem. Phys. Lett. 69*, 185−189.

Bourne, H. R., Sanders, D. A., & McCormick, F. (1991) *Nature 349*, 117−127.

Freissmuth, M., & Gilman, A. G. (1989) *J. Biol. Chem. 264*, 21907−21914.

Garrett, D. S., Lodi, P. J., Shamoo, Y., Williams, K. R., Clore, G. M., & Gronenborn, A. M. (1994) *Biochemistry 33*, 2852−2858.

Grzesiek, S., & Bax, A. (1992) *J. Am. Chem. Soc. 114*, 6291−6293.

Grzesiek, S., & Bax, A. (1993a) *J. Biomol. NMR 3*, 185−204.

Grzesiek, S., & Bax, A. (1993b) *J. Am. Chem. Soc. 115*, 12593−12594.

Ikura, M., Kay, L. E., & Bax, A. (1990) *Biochemistry 29*, 4659−4667.

Jurnak, F. (1985) *Science 230*, 32−36.

Kay, L. E., Keifer, P., & Saarinen, T. (1992) *J. Am. Chem. Soc. 114*, 10663−10665.

Kay, L. E., Xu, G.-Y., Singer, A. U., Muhandiram, D. R., & Forman-Kay, J. D. (1993) *J. Magn. Reson. B101*, 333−337.

Landis, C. A., Masters, S. B., Spada, A., Pace, A. M., Bourne, H. R., & Vallar, L. (1989) *Nature 340*, 692−696.

Lycksell, P.-O., Ingemarson, R., Davis, R., Gräslund, A., & Thelander, L. (1994) *Biochemistry 33*, 2838−2842.

Marion, D., Driscoll, P. C., Kay, L. E., Wingfield, P. T., Bax, A., Gronenborn, A. M., & Clore, G. M. (1989a) *Biochemistry 28*, 6150−6156.

Marion, D., Ikura, M., & Bax, A. (1989b) *J. Magn. Reson. 84*, 425−430.

Marion, D., Ikura, M., Tschudin, R., & Bax, A. (1989c) *J. Magn. Reson. 85*, 393−399.

Markby, D. W., Onrust, R., & Bourne, H. R. (1993) *Science 262*, 1895−1901.
Messerle, B. A., Wider, G., Otting, G., Weber, C., & Wüthrich, K. (1989) *J. Magn. Reson. 85*, 608−613.
Milburn, M. V., Tong, L., deVos, A. M., Brünger, A., Yamaizumi, Z., Nishimura, S., & Kim, S.-H. (1990) *Science 247*, 939−945.
Muhandiram, D. R., Farrow, N. A., Xu, G.-Y., Smallcombe, S., & Kay, L. E. (1993) *J. Magn. Reson. B102*, 317−321.
Noel, J. P., Hamm, H. E., & Sigler, P. B. (1993) *Nature 366*, 654−663.
Pai, E. F., Krengel, U., Petsko, G. A., Goody, R. S., Kabsch, W., & Wittinghofer, A. (1990) *EMBO J. 9*, 2351−2359.
Pascal, S. M., Muhandiram, D. R., Yamazaki, T., Forman-Kay, J. D., & Kay, L. E. (1994) *J. Magn. Reson. B 103*, 197−201.
Pontius, B. W. (1993) *Trends Biochem. Sci. 18*, 181−186.
Robishaw, J. D., Smigel, M. D., & Gilman, A. G. (1986) *J. Biol. Chem. 261*, 9587−9590.
Simon, M. I., Strathmann, M. P., & Gautam, N. (1991) *Science 252*, 802−808.
Spera, S., & Bax, A. (1991) *J. Am. Chem. Soc. 113*, 5490−5492.
Wishart, D. S., & Sykes, B. D. (1994) *J. Biomol. NMR 4*, 171−180.
Wishart, D. S., Richards, F. M., & Sykes, B. D. (1991) *J. Mol. Biol. 222*, 311−333.
Wittekind, M., & Mueller, L. (1993) *J. Magn. Reson. B 101*, 201−205.
Wüthrich, K. (1986) *NMR of Proteins and Nucleic Acids*, John Wiley, New York.
Zhu, G., & Bax, A. (1992) *J. Magn. Reson. 100*, 202−207.

BI941996R